Hollow Structures

DOI: 10.1002/anie.200907117

Synthesis of Cu_2O Nanoframes and Nanocages by Selective Oxidative Etching at Room Temperature**

Yongming Sui, Wuyou Fu, Yi Zeng, Haibin Yang, Yanyan Zhang, Hui Chen, Yixing Li, Minghui Li, and Guangtian Zou*

In recent years, hollow-structure particles (HSPs) have been widely studied due to their unique structures and potential applications. One successful synthetic strategy involves direct construction of HSPs from functional building blocks by processes such as the Kirkendall effect,[1] acid etching, coordination-polymer self-template-directed growth, and solid-state thermal decomposition process for the preparation of Cu_7S_4,[2] Fe_2O_3,[3] ZnO,[4] and MnO_2[5] HSPs. However, all of the reported HSPs require further heat- or acid-treatment processes, which have disadvantages such as increased costs and environmental pollution. Therefore, it remains a great challenge to develop a simple, mild (at room temperature), and environmentally friendly method for the one-pot synthesis of HSPs with well-defined shape.

Cu_2O is a typical p-type direct band gap semiconductor with a band gap of 2.17 eV and has potential applications in solar-energy conversion,[6] electrode materials,[7] sensors,[8] and catalysts.[9] Considerable effort has been devoted to obtaining hollow Cu_2O structure by employing techniques such as hydrothermal synthesis,[10] microemulsions,[11] template synthesis,[12] and acid etching.[13] Qi and co-workers prepared octahedral Cu_2O nanocages by Pd-catalytic reduction of an alkaline copper tartrate complex with glucose followed by a catalytic oxidation process.[14] More recently, truncated rhombic dodecahedral Cu_2O nanoframes and nanocages were synthesized by particle aggregation and acid etching.[13] In both synthetic processes, expensive and acidic or toxic solvents were used. Here we report a cheap and green synthetic route for Cu_2O nanoframes and nanocages with single-crystal walls. In our synthetic strategy, polyhedral Cu_2O particles were first prepared by adding a weak reducing agent (glucose) to a solution of copper citrate complex with polyvinylpyrrolidone (PVP) as capping agent,[15] and then Cu_2O nanoframes and nanocages were obtained in situ by oxidative etching at room temperature.

[*] Dr. Y. Sui, Prof. W. Fu, Prof. H. Yang, Dr. Y. Zhang, Dr. H. Chen, Y. Li, M. Li, Prof. G. Zou
State Key Laboratory of Superhard Materials
Jilin University, Changchun 130012 (China)
Fax: (+86) 431-8516-8763
E-mail: yanghb@jlu.edu.cn
Dr. Y. Zeng
State Key Laboratory on Integrated Optoelectronics
College of Electronic Science and Engineering
Jilin University, Changchun 130012 (China)

[**] We wish to thank Z. X. Guo for FESEM and HRTEM investigation of our samples.

Supporting information for this article is available on the WWW under http://dx.doi.org/10.1002/anie.200907117.

Perfect Cu_2O nanoframes were taken from the reaction mixture after the solution was exposed to air for 16 days at room temperature. Field-emission scanning electron microscopy (FESEM), transmission electron microscopy (TEM), and high-resolution TEM (HRTEM) images provided insight into the nanostructure and morphology of the Cu_2O nanoframes. As shown in Figure 1 A, the Cu_2O nanoframes are

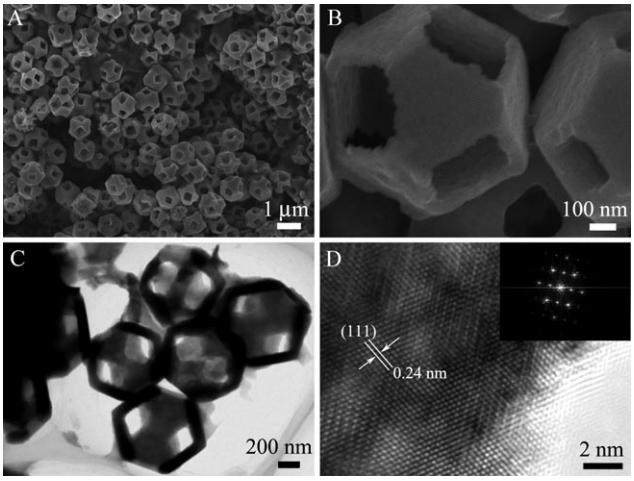

Figure 1. A) Low-magnification FESEM image of Cu_2O nanoframes. B) High-magnification FESEM image of a nanoframe. C) TEM image of Cu_2O nanoframes. D) Typical HRTEM image of a Cu_2O nanoframe. The inset of D) shows the corresponding FFT pattern.

relatively uniform in size. A single Cu_2O nanoframe is shown in Figure 1 B. The Cu_2O nanoframes, which have hollow interiors and high geometrical symmetry, are regular truncated octahedra with a mean edge length of about 300 nm. An important feature of the as-synthesized products is that most of the surface of the six {100} faces is absent. A truncated octahedral particle has eight hexagonal {111} faces and six {100} faces. Thus, the Cu_2O nanoframes are constructed of hexagonal {111} skeletons. The thickness of the nanoframe is about 60 nm. Consistent with FESEM observations, Figure 1 C shows a TEM image of Cu_2O nanoframes with hollow hexagonal shape; the average outer diameter of the Cu_2O nanoframes is about 700 nm. The HRTEM image confirms the single-crystal structure of the Cu_2O nanoframes. The fringes in a typical HRTEM image (Figue 1 D) are separated by about 0.24 nm, in good agreement with the (111) lattice spacing of Cu_2O. The inset of Figure 1 D shows the fast Fourier transform (FFT) pattern, which suggests that the Cu_2O nanoframe is a single-crystalline structure. Further-

more, the phase purity of the products was examined by X-ray diffraction (Figure S1, Supporting Information). All the peaks can be indexed to pure cubic phase Cu_2O (space group $Pn3m$, $a = 0.4294$ nm).

The formation process of the Cu_2O nanoframes was investigated in detail by characterizing the products obtained after different aging times. Figure 2 shows representative

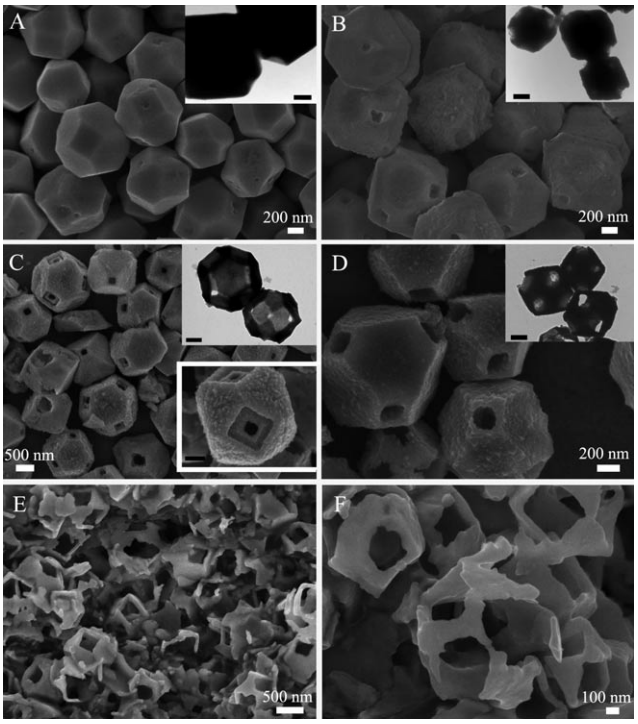

Figure 2. FESEM and TEM images of the nanoframes obtained at room temperature after aging for 1 (A), 4 (B), 8 (C), 12 (D), and 20 d (E, F). The insets of A, B, C, and D show the high-magnification TEM images and FESEM image, and the scale bar is 200 nm.

FESEM and TEM images of the products obtained at room temperature after 1, 4, 8, 12, and 20 d. As shown in Figure 2 A, small pits are observed on the {100} faces of the truncated octahedral particles after aging for 1 d. After aging for 4 d, truncated octahedral particles with some rough surfaces appear, which show holes on the {100} faces as well as pores in the interiors (Figure 2 B) indicating partial formation of hollow truncated octahedra. With increasing aging time, the interior of each truncated octahedron becomes increasingly empty, while the size of the hole in the surface starts to increase and form a frame with relatively thick walls (Figure 2 C). On gradual oxidative etching of the interior, the void further increases in size and the wall becomes thin after aging for 12 d (Figure 2 D). Notably, when the aging time is further prolonged, the truncated octahedral nanoframes are gradually etched into fragments (Figure 2 E and F). The Cu_2O particles totally dissolve after 24 d of aging to give a transparent, light blue solution, similar to the original reaction solution containing the copper citrate complex. As a result, the color of the reaction solution varies from deep red to light blue with increasing aging time (Figure S2, Supporting Information).

Based on the examination of the time-dependent formation of Cu_2O nanoframes, we propose that the nanoframes are formed by a two-step process: formation of the truncated octahedral Cu_2O precursor particles by reduction of the copper citrate complex with glucose, followed by subsequent hollowing of the truncated particles at room temperature by an oxidation process involving oxygen. During the hollowing step, the presence of oxygen is necessary for formation of the hollow structure. If the solution is purged with N_2 to remove dissolved O_2 prior to aging, the oxidative etching process can be effectively prevented. To analyze the synthesis process of the Cu_2O nanoframes, UV/Vis spectra of the solution at different stages of the reaction were recorded (Figure 3 A). The absorption peak at 735 nm can be attributed to copper citrate complex $[Cu_2(cit)_2]^{2-}$ ($cit^{3-} = [C_6O_7H_5]^{3-}$), and this assignment is consistent with the literature.[16] The change in the concentration of $[Cu_2(cit)_2]^{2-}$ could be followed by plotting the change in absorbance at about 735 nm against time (Figure 3 B). In the formation of precursor Cu_2O particles, $[Cu_2(cit)_2]^{2-}$ is reduced by glucose to generate Cu_2O particles and then large crystals. Hence, the concentration of $[Cu_2(cit)_2]^{2-}$ is gradually reduced in solution. During the hollowing step, the truncated octahedra are

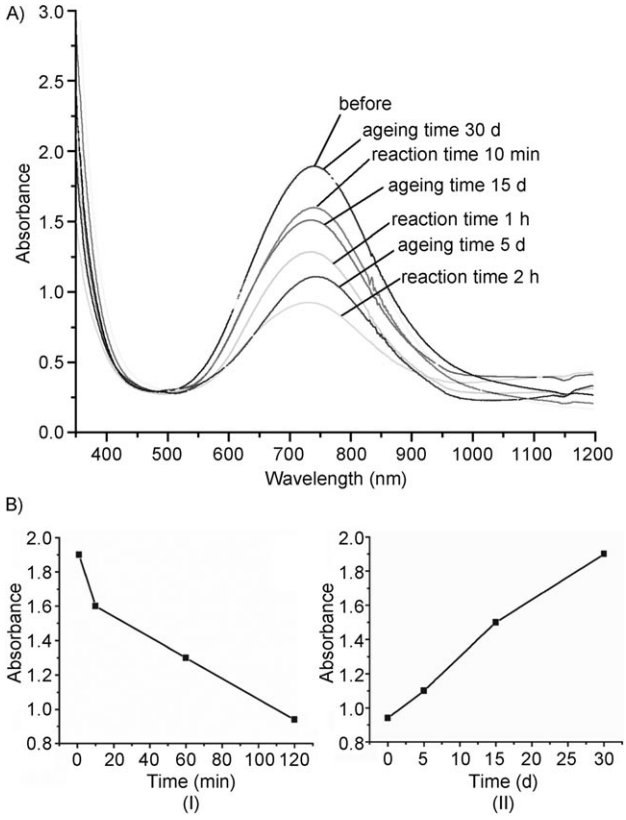

Figure 3. A) UV/Vis spectra of the solution taken at different reaction stages after removal of the Cu_2O particles by centrifugation. B) Time dependence of the absorbance at ca. 735 nm, which is directly proportional to the concentration of the $[Cu_2(cit)_2]^{2-}$ species. I) Formation of truncated octahedral particles. II) Formation of nanoframes. Note that the concentration of $[Cu_2(cit)_2]^{2-}$ increases as nanoframes are formed.

selectively etched on the {100} faces, and the concentration of $[Cu_2(cit)_2]^{2-}$ gradually increases. Finally, the concentration of $[Cu_2(cit)_2]^{2-}$ is largely consistent with that of the original solution. In the etching of the precursor Cu_2O particles, the following reactions may take place.

Formation of $[Cu_2(cit)_2]^{2-}$ [Eq. (1)] forces Equation (2) toward the right-hand side and speeds up dissolution of the Cu_2O particles. Overall, the Cu_2O hollow nanoframes are obtained by the balance between two opposing reactions: reduction of Cu^{2+} ($[Cu_2(cit)_2]^{2-}$) to form Cu^+ (Cu_2O), and oxidation of Cu^+ to Cu^{2+} species. A similar process was observed in corrosion-based synthesis of single-crystal Pd nanoboxes.[17] Furthermore, Na^+ in sodium citrate and sodium carbonate is not responsible for the formation of hollow nanoframes. When potassium citrate and potassium carbonate are used instead of sodium citrate and sodium carbonate in the synthesis, the nanoframes still can be obtained (Figure S3, Supporting Information).

$$2\,Cu^{2+} + 2\,cit^{3-} \rightarrow [Cu_2(cit)_2]^{2-} \quad (1)$$

$$2\,Cu_2O + O_2 + 4\,H_2O \rightarrow 4\,Cu^{2+} + 8\,OH^- \quad (2)$$

Generally, when organic or inorganic additives are added during the crystal growth process, the relative order of surface energies can be modified. The growth control of Cu_2O crystals by adsorption of PVP has been extensively studied.[18] Our investigations show that PVP adsorption on the Cu_2O surface takes place, and that the adsorbed PVP cannot be removed by washing (Figure S4, Supporting Information). In a Cu_2O typical unit, each O is surrounded by a tetrahedron of Cu, and each Cu has two O neighbors.[19] For {111} planes, every other Cu atom has a dangling bond perpendicular to the {111} planes, whereas for {100} and {110} planes, O- and -O-Cu-O-Cu-terminated surfaces are present, respectively.[18] Therefore, the coordinatively unsaturated Cu in the {111} face is obviously more active for interaction with PVP. To prove this hypothesis, ethanol was added to the solution and aging was carried out at room temperature for 4 d. Selective etching of the {100} faces was disrupted, and random etching of the imperfect nanoframes can occur, as shown in Figure S5 (Supporting Information. The PVP molecules should be adsorbed preferentially on the {111} faces of the Cu_2O particles, and the layer of adsorbed PVP molecules on the {111} surfaces may be temporarily disrupted by added ethanol. Strong adsorption of polymers or foreign ions on the surfaces of particles can effectively block oxidative etching.[20] Thus, PVP may play the role of protecting the {111} faces from direct etching, whereas the removal of PVP facilitates the oxidative etching reaction between Cu_2O and O_2 to form $[Cu_2(cit)_2]^{2-}$. This suggests that the surfactant PVP is significant for the synthesis of Cu_2O nanoframes.

This method of oxidative etching coupled with templating of the precursor particles can be extended to morphology-preserved synthesis of hollow structures with morphologies other than polyhedra. Different structures and morphologies of Cu_2O precursor particles could be obtained simply by changing the PVP concentration in our synthesis system (Figure S6 and Table S1, Supporting Information). As expected, nanocages with holes on the apexes could be obtained at room temperature (Figure 4; Table S1 and Figure S7, Supporting Information). This formation process

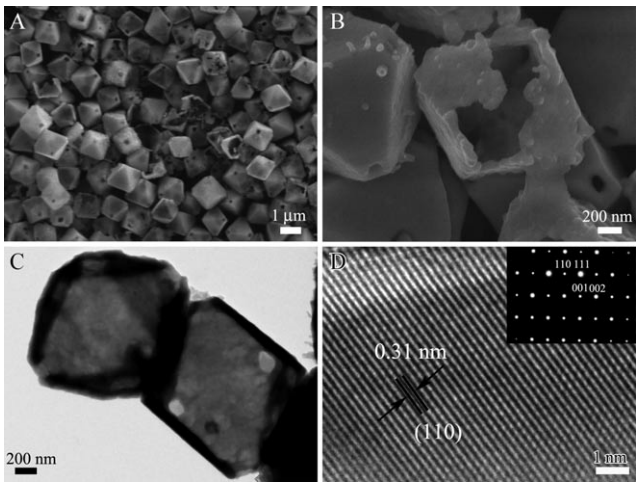

Figure 4. A) Low-magnification FESEM image of the Cu_2O nanocages obtained at room temperature after 24 d. B) High-magnification FESEM image of the nanocages. C) TEM image of the Cu_2O nanocages. D) Typical HRTEM image taken from a Cu_2O nanocage. The inset of D) shows the SAED pattern.

is analogous to the reported formation of octahedral Cu_2O nanocages, which etching occurs from the apex of octahedra to form octahedral nanocages.[14] In addition, imperfect hollow cubes and hollow nanocages were prepared by oxidative etching of cubic and octahedral Cu_2O precursor particles by a similar strategy (Supporting Information, Table S1, Figures S8 and S9). In our experiments, cubes bounded by six equivalent {100} faces are formed when the ratio R between the growth rates along the {100} and {111} directions is 0.58, and octahedra bounded by eight equivalent {111} faces will result if R is increased to 1.73 (Table S1 and Figure S6, Supporting Information). Thus, if the selectively etched crystal face is absent, overetching can occur and leads to formation of imperfect hollow structures. These results confirm that such shape-preserved formation of hollow structures is limited to the Cu_2O/citrate system, and that cubic and octahedral Cu_2O particles are not beneficial for the formation of hollow structure.

To determine the relative photocatalytic activities of the Cu_2O particles, rhodamine B was used for photodegradation experiments. As illustrated in Figure S10 (Supporting Information), octahedral Cu_2O particles with exclusively {111} faces exhibited superior photoactivities over octahedral particles with truncated corners due to surface properties. Huang et al. reported that the {111} face of Cu_2O contains surface copper atoms with dangling bonds, so that the {111} faces are higher in surface energy and expected to be more catalytically active than the {100} faces.[21] Whether solid or hollow, the photocatalytic activity of truncated octahedral ($R = 1.15$) particles is higher than that of the truncated octahedra with $R = 1$. This result further suggests that Cu_2O particles with more {111} facets can serve as more efficient

photocatalysts. Moreover, the photocatalytic activity of hollow particles is higher than that of the solid particles. This can be attributed to the hollow structure and larger surface area. The hollow structure can allow multiple reflection of light within the interior hollow and lead to more efficient use of light and improved photocatalytic activity of Cu_2O.

In summary, well-defined Cu_2O nanoframes and nanocages with high geometrical symmetry have been readily fabricated in situ by oxidative etching coupled with templating of the precursor particles. More specifically, etching and shape preservation could be combined to transform single-crystal Cu_2O truncated octahedra into nanoframes and nanocages in a one-pot synthesis without the involvement of exotic templates. Our results also demonstrated that PVP acts as a capping agent, and that preferential adsorption on the {111} faces of the Cu_2O crystals "freezes" the {111} planes to facilitate the formation of hollow structures. The Cu_2O nanoframes and nanocages with controllable wall thickness and pore size could find applications in various areas, including catalysis and material encapsulators or carriers. Furthermore, this strategy may be extended to other metal oxide systems and could possibly be used for device fabrication with appropriate metal oxide/complex combinations.

Experimental Section

In a typical procedure, an aqueous solution was first prepared by mixing 17 mL of water, 1 mL of 0.68 M copper sulfate, and PVP (0.9 g, K-30, $M_w = 30000$) in a round-bottomed glass flask. The mixture was stirred with a magnetic stirrer for about 15–20 min, and then 1 mL of 0.74 M sodium citrate and 1.2 M anhydrous sodium carbonate mixed solution was added in dropwise manner. A dark blue color soon appeared, but no precipitate was observed. After about 10 min, 1 mL of 1.4 M glucose solution was slowly dropped into this solution. The solution was kept in a water bath at 80 °C for 2 h, and then allowed to cool to room temperature. The resulting solution was then exposed to air and allowed to age for up to 16 d at room temperature (ca. 20 °C). The orange precipitate was collected by filtration, washed several times with distilled water and absolute alcohol, and finally dried in vacuum at 60 °C for 8 h. Further experiments were also conducted under different conditions by using procedures similar to those presented above (for detailed experimental conditions, see Table S1 of the Supporting Information).

X-ray powder diffraction (XRD) analysis was conducted on a Rigaku D/max-2500 X-ray diffractometer with $Cu_{K\alpha}$ radiation ($\lambda =$ 1.5418 Å). FESEM images were recorded on a JEOL JEM-6700F microscope operating at 5 kV. TEM images, SAED patterns, and HRTEM images were obtained on a JEOL JEM-2000EX microscope with accelerating voltage of 200 kV and a JEOL JEM-3010 microscope operated at 200 kV, respectively. UV/Vis absorption spectra were recorded on a spectrophotometer (Shimadsu 3100 UV-VIS-NIR). FTIR data were taken on an MPA NIR spectrometer.

The photocatalytic activity of the Cu_2O particles was evaluated by degradation of rhodamine B under UV/Vis irradiation from a 200 W Hg lamp. 0.1 g samples of Cu_2O particles with different morphologies were dispersed in a 50 mL of aqueous rhodamine B solution (15 mg L^{-1}). After magnetic stirring in the dark for 30 min to reach adsorption equilibrium, the solution was exposed to photoirradiation. Concentrations of rhodamine B were carried measured by UV/Vis spectroscopy every 60 min.

Received: December 17, 2009
Revised: February 26, 2010
Published online: May 5, 2010

Keywords: nanoparticles · nanostructures · oxidative etching · oxides · photocatalysts

[1] Y. Yin, R. Rioux, C. K. Erdonmcz, S. Hushes, G. A. Somorjai, A. P. Alivisatos, *Science* **2004**, *304*, 711.
[2] H. L. Cao, X. F. Qian, C. Wang, X. D. Ma, J. Yin, Z. K. Zhu, *J. Am. Chem. Soc.* **2005**, *127*, 16024.
[3] K. An, S. G. Kwon, M. Park, H. B. Na, S. Baik, J. H. Yu, D. Kim, J. S. Son, Y. W. Kim, I. C. Song, W. K. Moon, H. M. Park, T. Hyeon, *Nano Lett.* **2008**, *8*, 4252.
[4] S. Jung, W. Cho, H. J. Lee, M. Oh, *Angew. Chem.* **2009**, *121*, 1487; *Angew. Chem. Int. Ed.* **2009**, *48*, 1459.
[5] a) J. B. Fei, Y. Cui, X. H. Yan, W. Qi, Y. Yang, K. W. Wang, Q. He, J. B. Li, *Adv. Mater.* **2008**, *20*, 452; b) L. Z. Wang, F. Q. Tang, K. Ozawa, Z. G. Chen, A. Mukher, Y. C. Zhu, J. Zou, H. M. Cheng, G. Q. Lu, *Angew. Chem.* **2009**, *121*, 7182; *Angew. Chem. Int. Ed.* **2009**, *48*, 7048.
[6] A. O. Musa, T. Akomolafe, M. J. Carter, *Sol. Energy Mater. Sol. Cells* **1998**, *51*, 305.
[7] P. Poizot, S. Laruelle, S. Grugeon, L. Dupont, J. M. Taracon, *Nature* **2000**, *407*, 496.
[8] J. Zhang, J. Liu, Q. Peng, X. Wang, Y. Li, *Chem. Mater.* **2006**, *18*, 867.
[9] a) H. Zhang, X. Ren, Z. L. Cui, *J. Cryst. Growth* **2007**, *304*, 206; b) B. White, M. Yin, A. Hall, D. Le, S. T. Stolbov, Rahman, N. Turro, S. O'Brien, *Nano Lett.* **2006**, *6*, 2095.
[10] a) Y. Chang, J. T. Teo, H. C. Zeng, *Langmuir* **2005**, *21*, 1074; b) J. T. Teo, Y. Chang, H. C. Zeng, *Langmuir* **2006**, *22*, 7369.
[11] Q. D. Chen, X. H. Shen, H. C. Gao, *J. Colloid Interface Sci.* **2007**, *312*, 272.
[12] H. L. Xu, W. Z. Wang, *Angew. Chem.* **2007**, *119*, 1511; *Angew. Chem. Int. Ed.* **2007**, *46*, 1489.
[13] C. H. Kuo, M. H. Huang, *J. Am. Chem. Soc.* **2008**, *130*, 12815.
[14] C. H. Lu, L. M. Qi, J. H. Yang, X. Y. Wang, D. Y. Zhang, J. L. Xie, J. M. Ma, *Adv. Mater.* **2005**, *17*, 2562.
[15] Y. M. Sui, W. Y. Fu, H. B. Yang, Y. Zeng, Q. Zhao, Y. G. Li, X. M. Zhou, Y. Leng, M. H. Li, G. T. Zou, *Cryst. Growth Des.* **2010**, *10*, 99.
[16] P. G. Daniele, G. Ogtacol, O. Zerbinati, *Transition Met. Chem.* **1988**, *13*, 87.
[17] Y. J. Xiong, B. Wiley, J. Y. Chen, Z. Y. Li, Y. D. Yin, Y. N. Xia, *Angew. Chem.* **2005**, *117*, 8127; *Angew. Chem. Int. Ed.* **2005**, *44*, 7913.
[18] D. Y. Zhang, H. Zhang, L. Guo, K. Zhang, X. D. Han, Z. Zhang, *J. Mater. Chem.* **2009**, *19*, 5220.
[19] R. Restori, D. Schwarzenbach, *Acta Crystallogr. Sect. B* **1986**, *42*, 201.
[20] a) Y. J. Xiong, J. M. McLellan, Y. D. Yin, Y. N. Xia, *Angew. Chem.* **2007**, *119*, 804; *Angew. Chem. Int. Ed.* **2007**, *46*, 790; b) B. Lim, Y. J. Xiong, Y. N. Xia, *Angew. Chem.* **2007**, *119*, 9439; *Angew. Chem. Int. Ed.* **2007**, *46*, 9279; c) C. C. Li, R. Sato, M. Kanehara, H. B. Zeng, Y. Bando, T. Teranishi, *Angew. Chem.* **2009**, *121*, 7015; *Angew. Chem. Int. Ed.* **2009**, *48*, 6883.
[21] a) C. H. Kuo, M. H. Huang, *J. Phys. Chem. C* **2008**, *112*, 18315; b) J. Y. Ho, M. H. Huang, *J. Phys. Chem. C* **2008**, *113*, 14159.

